UC Santa Barbara
UC Santa Barbara Previously Published Works

Title

A new climatology for Southern Hemisphere blockings in the winter and the combined effect of ENSO and SAM phases

Permalink

https://escholarship.org/uc/item/5913c9j2

Journal

International Journal of Climatology, 34(5)

ISSN

0899-8418

Authors

Oliveira, Flavio NM
Carvalho, Leila MV
Ambrizzi, Tercio

Publication Date

2014-04-01

DOI

10.1002/joc.3795

Peer reviewed

A new climatology for Southern Hemisphere blockings in the winter and the combined effect of ENSO and SAM phases

Flavio N. M. Oliveira,[a,b]* Leila M. V. Carvalho[c,d] and Tercio Ambrizzi[a]

[a] *Department of Atmospheric Sciences, University of São Paulo, Brazil*
[b] *1° District of Meteorology, National Institute of Meteorology, Manaus, Brazil*
[c] *Department of Geography, University of California, Santa Barbara, USA*
[d] *Earth Research Institute, University of California, Santa Barbara, USA*

ABSTRACT: This study presents 53-year climatology of Southern Hemisphere (SH) blockings in the winter using daily 500-hPa geopotential height data from NCEP–NCAR reanalysis. The variability of SH blocking events and their relationships with combined phases of El Niño/southern oscillation (ENSO) and the southern annular mode (SAM) are examined. Conventional indices were revised and a slightly modified index is proposed to detect latitudinal variations of SH blockings. The South Pacific region is examined in detail. There is no statistically significant long-term trend in the SH blockings. During moderate El Niño, the preferred location SH blocking is observed over East Pacific, and we show that the blocking frequency increases during negative SAM phases. During moderate La Niña the SH blockings are significantly suppressed over Central Pacific, with lower blocking frequency during positive SAM phases. These results indicate that the daily variability of SH blocking is strongly modulated by both ENSO and SAM phases.

KEY WORDS   blocking; El Niño/southern oscillation; Antarctic oscillation; austral winter

Received 16 January 2011; Revised 20 June 2013; Accepted 2 July 2013

1. Introduction

Blocking events often result from a strong meridional deformation of mid-latitude flows causing the main jet stream to be divided into two branches. They are observed as anomalous and persistent high-pressure centre that obstructs the typical large-scale zonal flow pattern. Several theories have been proposed in the last 60 years to explain the occurrence of blocking events (Elliot and Smith, 1949; Rex, 1950b; Lejenäs and Økland, 1983; Dole, 1986; Barry and Chorley, 1992; Colucci and Alberta, 1996). Nevertheless, the mechanisms of formation and dissipation of blocking events need to be further understood. These mechanisms appear to involve nonlinear interactions between the transient eddies and the seasonal mean circulation that depend on the teleconnection patterns (Kalnay-Rivas and Merkine, 1981; Frederiksen, 1982; Shutts, 1983; Blackmon *et al.*, 1986; Mullen, 1987; Lupo, 1997; Renwick, 1998; Nascimento and Ambrizzi, 2002).

Early studies have used subjective techniques to detect blockings in the Southern Hemisphere (SH) based on kinetic properties of the blocking flow structure on surface and mid-troposphere (Van Loon, 1956; Wright,

1974; Casarin, 1983). Following this criterion, a blocking structure can be identified by the split of the jet into subtropical and polar branches in the mid-troposphere and by the quasi-stationary structure. According to these methods, blocking events should last at least 6 days. Recent and more objective methods have modified these criteria by considering shorter lifetimes and new extensions (e.g. Tibaldi *et al.*, 1994, hereafter T94; Sinclair, 1996; Berrisford *et al.*, 2006). These objective methods have been proposed in the late 1970s and focused primarily on the Northern Hemisphere (NH) (Charney *et al.*, 1981; Dole and Gordon, 1983; Dole, 1986) where blockings are detected as persistent positive height anomalies in the mid-troposheric flow.

For the SH, the first combined technique (subjective and objective) was originally proposed by Lejenäs (1984), in which the criterion derived from the kinetic properties of the flow was quantified using the well-established concept of the zonal index (Namias, 1947). For instance, for a certain longitude to be blocked, Lejenäs (1984) required easterly latitudinal zonal wind average. In other words, the height difference between 35° and 55°S should be less than zero, that is:

$$Z(\lambda)_{\phi_N} - Z(\lambda)_{\phi_S} < 0 \qquad (1)$$

where Z and λ, are 500-hPa geopotential height and longitude, respectively. ϕ_N and ϕ_S are constant latitudes at 35°S and 55°S. This index is proportional to the zonal

* Correspondence to: 1° District of Meteorology, National Institute of Meteorology, Avenida Mario Ypiranga, 1041, Manaus, AM 69057-001, Brazil. E-mail: flavio.natal@inmet.gov.br

geostrophic wind component and provides a measure of the zonal flow intensity for each longitude. Only a decade later, T94 found that cold cutoff lows anomalously displaced toward polar latitudes could also result in negative values in the basic criterion of Lejenäs (1984). To solve this problem, T94 proposed a slightly modified version of Lejenäs (1984), as follows: (1) they added two values of 500-hPa geopotential height gradient (that is essentially equivalent to the condition 1 alone) and (2) they added a negative geopotential height gradient southward of 50°S, in order to exclude non-blocked longitudes, according to Equation (2):

$$\frac{[Z(\lambda, \phi_0 - \Delta\phi) - Z(\lambda, \phi_0)]}{[(\phi_0 - \Delta\phi) - (\phi_0)]} < -10 \ \text{gpm} \quad (2)$$

where Z, λ and ϕ_0 are 500-hPa height geopotential, longitude and the central constant latitude at 50°S, respectively. Different from Lejenäs (1984), $\phi_0 - \Delta\phi$ allows for some variation on the latitude. Some versions of the T94 method have been largely used in several other studies to detect blocking events (e.g. Trigo *et al.*, 2004; Barriopedro *et al.*, 2006; Damião *et al.*, 2008; Matsueda *et al.*, 2010; Oliveira, 2011). Similarly, this study is based on the T94 method. A few other objective techniques have been proposed, such as those based on the difference of potential temperature in the dynamic tropopause known as the PV-θ blocking index (Hoskins *et al.*, 1985) or automated procedures for locating and tracking of high-pressure centres (e.g. Sinclair, 1996).

There has been some consensus among several studies focusing on the SH: (1) SH blockings are concentrated in the South Pacific with maximum frequency during the winter and peaks in the west and east Pacific (Sinclair, 1996; Berrisford *et al.*, 2006); (2) blockings are usually located at lower latitudes and are less frequent comparatively to the NH blockings (e.g. Tibaldi *et al.*, 1994), and (3) the existence of intense westerly winds in the mid and high troposphere significantly reduces the SH blocking duration (e.g. Trenberth and Mo, 1985; Berrisford *et al.*, 2006). Moreover, some studies have found a new region with high frequency of blocking over Southeast Pacific (e.g. Rutllant and Fuenzalida, 1991; Sinclair, 1996).

Furthermore, a few previous studies have examined the relationships between SH blocking and El Niño/southern oscillation (ENSO) (Rutllant and Fuenzalida, 1991; Renwick, 1998; Marques and Rao, 2000; Wiedenmann *et al.*, 2002). They found a relatively higher frequency of SH blocking events over Southeast Pacific during El Niño years. Also, they described the main characteristics of the SH blocking events in terms of frequency, duration and preferred regions. However, some of them were limited to small datasets (e.g. Rutllant and Fuenzalida, 1991), focused on specific cases (Marques and Rao, 2000), examined the South Pacific as a single sector (e.g. Wiedenmann *et al.*, 2002) and some did not compare the opposite ENSO phases against neutral phases (e.g. Renwick, 1998). Finally, no previous study has investigated in detail the relationships between blockings stratified

into ENSO categories or used a dataset longer than 30 years. Nevertheless, according to previous results, the high-frequency dynamics accounts for more than 75% of the observed amplification for the North Pacific blockings (e.g. Nakamura *et al.*, 1997), showing that this relationship between ENSO and SH blockings requires a more detailed investigation.

Southern annular mode (SAM) is considered the main mode of variability of the extratropics of the SH (Gong and Wang, 1999; Thompson and Wallace, 2000), and is related to the extratropical storm tracks and jet stream variability (e.g. Hartmann and Lo, 1988; Limpasuvan and Hartmann, 2000). Therefore, it is reasonable to hypothesize that SAM plays a significant role in modulating the SH blocking variability. For instance, Carvalho *et al.* (2005) have shown the importance of tropical–extratropical interactions for variations of the SAM and the respective changes in the upper level circulation. Fogt *et al.* (2010) showed that teleconnections in the Southern Pacific are strengthened depending on the phase combination between ENSO and SAM. Thus, this study will further explore how ENSO and SAM phases modulate blockings in the SH.

The main goal of this article is to provide a new climatology of SH blockings during the winter and their interannual variability. A slightly modified version of T94 index is proposed to investigate SH blockings in extratropical regions and we divide the Pacific Ocean into several sectors. In addition, we examine the spatial and temporal variability of these events and relationships with the ENSO according to the episode's intensity and with respect to SAM.

This article is organized as follows. Section 2 presents datasets and discusses the blocking index used in this analysis. Section 3 presents a comparison with a standard blocking index. Section 4 presents the climatology of SH blockings with focus on their variability during ENSO phases. Section 5 investigates trends in SH blocking events. Section 6 discusses and explores the combined influence of SAM and ENSO on the interannual variability of SH blockings. Conclusions are presented in Section 7.

2. Data and methodology

This study uses 53-years (1958–2010) of daily mean 500-hPa geopotential height (H500, $2.5 \times 2.5°$ spatial resolution) from the National Center of Environmental Prediction–National Center for Atmospheric Research (NCEP/NCAR) reanalysis (Kalnay *et al.*, 1996; Kistler *et al.*, 2001).

Although the NCEP–NCAR reanalysis begins in 1948 and extends until the present, caution should be exerted when interpreting long-term trends in upper air variables, in particular in the SH. For instance, according to Kistler *et al.* (2001) the NCEP–NCAR reanalyses are less reliable between 1949 and 1957 due to the scarce number of upper-air data observations in the SH.

After 1957, a modern rawinsonde network was established, primarily in the NH, and in 1979 the modern satellite era began. According to Hines *et al.* (2000), these changes could result in jumps and long-term trends when using NCEP–NCAR reanalysis from the beginning of the reanalysis until the present date.

To investigate these issues further and how they have affected H500 in the SH, we examined the seasonal mean of H500 in two regions: mid-latitudes (35°S–50°S) and mid-high latitudes (55°S–70°S) and over two longitudes 180° and 130°W. As we will discuss in the following sections, these regions were chosen due to the non-stationary behaviour of the frequency of blockings. To perform these analyses we used the method to detect change points in climatic regimes developed by Rodionov (2006). The method is based on a sequential data processing technique which tests differences in the mean between two data segments of length L. Using $L = 10$ (equivalent to 10 seasons) and significance of 5% the method indicates a change point in 1957 over mid-latitudes, which coincides with the period when the modern rawinsonde network began (Figure 1(c)). This regime extends until 1974. In mid-high latitudes, we observed a change point in 1967 and 1986 (Figure 7(d)). There was no change point in H500 detected with the Rodionov (2006) method at the date line (Figure 1(a)). Interestingly, there was no change point separating the period before and after the beginning of the satellite era (1979) in all regions examined with the Rodionov (2006) method. It is important to emphasize that change points are not necessarily related to data quality; climatic regime shifts have been associated with modes that vary on decadal to multi-decadal time scales such as the Pacific Decadal Oscillation (Rodionov, 2006; Carvalho *et al.*, 2011). Based on these results this study investigates the climatology of blockings using NCEP–NCAR reanalysis after 1957, when a well-known change in observational network has been documented (Kistler *et al.*, 2001).

2.1. Blocking index

The blocking index $B(\lambda)$ used here is a slightly modified version of T94 adapted to the relatively higher horizontal resolution of NCEP–NCAR reanalysis ($2.5 \times 2.5°$, instead of $3.75 \times 3.75°$ used by T94) and stratified in three latitude bands (see below). For instance, according to T94 method, two H500 gradients GHGS and GHGN should be calculated simultaneously for every longitude (λ) at each one of the three reference latitudes, as follows:

$$\text{GHGN} = \frac{Z(\lambda, \phi_0) - Z(\lambda, \phi_N)}{\phi_0 - \phi_N} < 0 \qquad (3a)$$

$$\text{GHGS} = \frac{Z(\lambda, \phi_S) - Z(\lambda, \phi_0)}{\phi_S - \phi_0} < 0 - 10 m/°\text{lat} \quad (3b)$$

where $\phi_N = 35°S + \Delta$, $\phi_0 = 50°S + \Delta$, $\phi_S = 65°S + \Delta$ and $\Delta = 0, \pm 5$ (to allow some variation northward and southward direction from each reference latitude). The condition 3b is identical to Equation (2). Other authors

(e.g. Trigo *et al.*, 2004; Barriopedro *et al.*, 2006) have performed similar procedure; however, here we computed separately the blocking index at low-latitudes [ϕ_l], mid-latitudes [ϕ_m] and high-latitudes [ϕ_h] for every longitude (λ), as follows:

$$\begin{cases} \text{GHGN}(\lambda, \phi_l) = \frac{Z(\lambda, \phi_l) - Z(\lambda, \phi_{30°S})}{\phi_l - \phi_{30°S}} \\ \text{GHGN}(\lambda, \phi_m) = \frac{Z(\lambda, \phi_m) - Z(\lambda, \phi_N)}{\phi_m - \phi_N} \\ \text{GHGN}(\lambda, \phi_h) = \frac{Z(\lambda, \phi_h) - Z(\lambda, \phi_{40°S})}{\phi_h - \phi_{40°S}} \end{cases} \qquad (4a)$$

$$\begin{cases} \text{GHGS}(\lambda, \phi_l) = \frac{Z(\lambda, \phi_{60°}) - Z(\lambda, \phi_l)}{\phi_{60°} - \phi_l} \\ \text{GHGS}(\lambda, \phi_m) = \frac{Z(\lambda, \phi_S) - Z(\lambda, \phi_m)}{\phi_S - \phi_m} \\ \text{GHGS}(\lambda, \phi_h) = \frac{Z(\lambda, \phi_{70°S}) - Z(\lambda, \phi_h)}{\phi_{70°S} - \phi_h} \end{cases} \qquad (4b)$$

where $\phi_l = 45°S$, $\phi_m = 50°S + \Delta$, $\phi_h = 55°S$, $\phi_N = 30°S + \Delta$, $\phi_S = 65°S + \Delta$ and $\Delta = 0, \pm 2.5$ (to allow some variation for the reference latitude at mid-latitudes).

Also, the total range of latitudes is computed taking into account only GHGN(λ, ϕ_m) and GHGS(λ, ϕ_m), basically by setting $\Delta = 0, \pm 2.5$, or ± 5. This approach provides a measure for the total number of blocked longitudes. Here, Δ is called delta range and is used to allow some latitudinal variation around the reference latitudes. There are three (five) values of Δ for detections at mid-latitudes (total range of latitudes), whereas at mid-low and mid-high latitudes belt the method does not allow variations in latitude. Thus, the mid-low and mid-high reference latitudes are always constant. GHGN can be interpreted as the geopotential height gradient or the blocking strength in meters per degree of latitude. GHGS is the geopotential height gradient at high-latitudes, a condition imposed by T94 to ensure the exclusion of non-blocked longitudes, as discussed in Section 1. Thus, a given longitude (λ) is considered blocked when both GHGN and GHGS verify simultaneously the condition expressed by Equation (5) for a least one range of Δ.

$$B(\lambda) = \text{GHGN} > 0, \text{ if GHGS} < -10 \text{ gpm}/°\text{lat.} \quad (5)$$

Moreover, the procedure incorporates five Δ values instead of the three proposed by T94. Barriopedro *et al.* (2006) suggested that the use of five Δ values detect more blocked longitudes than the three Δ values proposed by T94. Therefore, the five Δ values and higher horizontal grid resolution (2.5×2.5) in this study represent improvements to the standard method of T94. Table I summarizes the boundaries of these latitudinal belts. Note that the latitudinal range between mid-low and mid-high bands is about $10°$, a reasonable range to detect synoptic systems (>1000 km). The advantage of the method proposed here, which examines three reference latitudes, is to obtain a more realistic climatology of blocked longitudes varying between low and high latitudes, as well as the frequency, preferred locations and the timescale of blocking events.
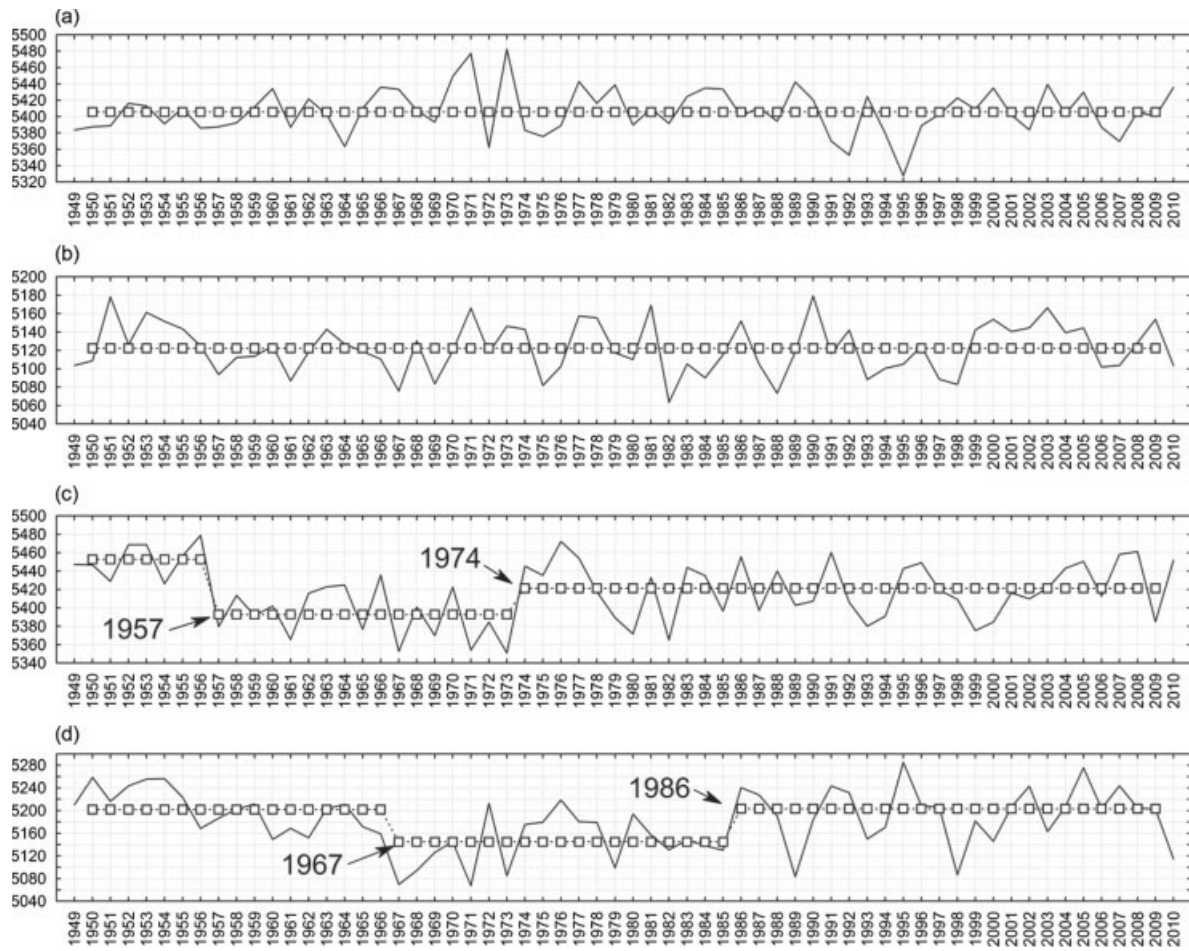
Figure 1. Mean fields of 500-hPa geopotential height (solid lines) with a stepwise trend (squared lines) for 180° of longitude at (a) mid-latitudes (35°S–50°S) and (b) mid-high latitudes (55°S–70°S) and for 135° of longitude at (c) mid-latitudes (35°S–50°S) and (d) mid-high latitudes (55°S–70°S) from the period 1950 to 2010.

Table I. Reference latitudes properties of blocking index.

Reference latitudes	Number of delta ranges	Latitudinal boundaries
Mid-low $(\lambda, \phi l)$, $\phi l = 45°S$	1	30.0°S–45.0°S
Mid-low $(\lambda, \phi m)$, $\phi m = 50°S$	3	32.5°S–52.5°S
Mid-high $(\lambda, \phi h)$, $\phi h = 55°S$	1	40.0°S–55.0°S
Total range	5	30.0°S–55.0°S

The criterion discussed in Equation (5) does not take into account the longitudinal extent and the timescale. Here, we consider a 'blocking event' when the contiguous blocked longitude extends at least 15°, including the longitude λ. Note that the minimum spatial extent required in this criterion corresponds to about 1200 and 1100 km at ϕ_E and ϕ_P, respectively and these values are greater than the Rossby radius of deformation. Also, we used a timescale of 3 days to define a blocking event, following Sinclair (1996) and Marques and Rao (1998). As discussed in Section 4, the timescale of 3 or 4 days is more appropriate for the SH than 5 days commonly used in previous studies (Tibaldi *et al.*, 1994; Renwick, 1998, Wiedenmann

et al., 2002). Since thresholds are somewhat arbitrary, if in a sequence of *n* days the criterion fails in one day but is fulfilled in the next day(s) we assume the duration of the event to be the total number of *n* days in the sequence, including the day when the criterion failed. In other words, one event is considered independent from another if they are at least 2 or more days apart.

2.2. Sectors of occurrence of blocking events

Previous studies have shown that blocked longitudes are more frequent in some specific regions in the SH (Van Loon, 1956; Lejenäs, 1984; Tibaldi *et al.*, 1994; Sinclair, 1996; Marques, 1996). However, these blockings may not be completely stationary and may experience some small zonal and meridional displacement. In this study, to properly address the spatial variability of blocked longitudes and blocking events, the South Pacific Ocean was divided into five sectors: East Indian (EIN), West Pacific (WPA), Central Pacific (CPA), East Pacific (EPA) and West Atlantic (WAT). The sectors WPA, CPA and EPA are examined in detail. Table II summarizes the longitudinal extent of the sectors considered in this study and the reasons for this separation are clarified in Section 4.
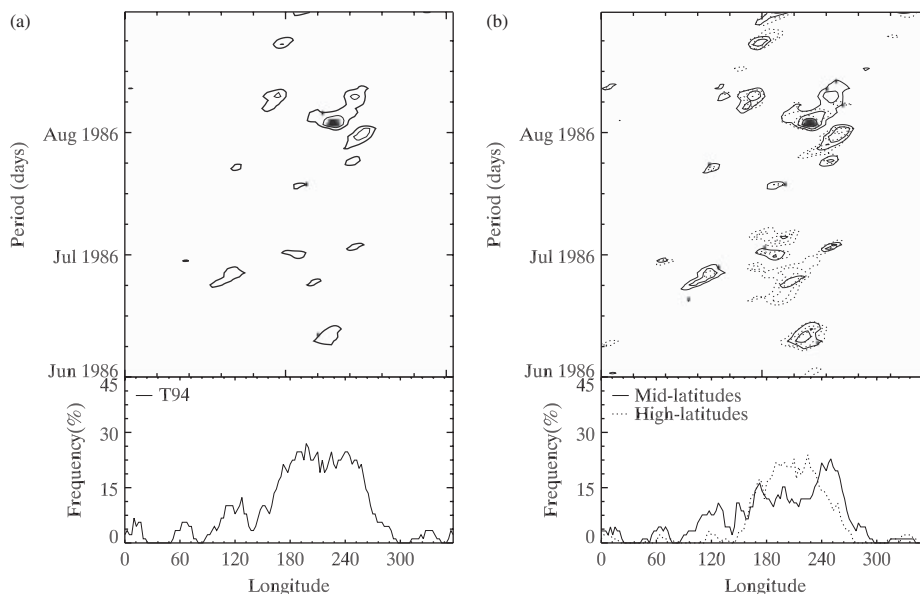
Figure 2. Hovmöller diagrams (longitude-time) of the strength of the blocking flows (m/° latitude) and their respective frequencies per longitude for the austral winter of 1986: (a) T94 scheme; (b) mid-latitude (solid lines) and mid-high (dotted lines) latitude references of blocking index (see text for further details).

Table II. Sectors of blocking events, acronyms and longitudinal boundaries.

Sector	Acronym	Longitudinal boundaries
East Indian	EIN	090.0°E–127.5°E
West Pacific	WPA	130.0°E–180.0°S
Central Pacific	CPA	177.5°E–120.0°E
East Pacific	EPA	117.5°E–80.0°E
West Atlantic	WAT	077.5°E–40.0°E

3. Comparison with the T94 blocking index

A few previous studies using a modified T94 version have used a Hovmöller diagram to show the performance of the blocking index. However, these studies did not properly address whether the northern geopotential gradient (GHGN) in a Hovmöller diagram represents the maximum or the average gradient within a range of latitudes. Since the main purpose of our index is to show how blocking events vary in latitude, we adopted the 'averaged' GHGN over mid-latitudes. For instance, if a blocking event only occurs at high latitudes, the averaged GHGN will be weak or less than zero at the lowest latitudes, whereas the GHGN will be strong at high latitudes. Thus, the preferred latitude will appear in a Hovmöller diagram.

The well-documented winter of 1986 (Marques and Rao, 2001) was used here to exemplify the application of the method at each reference latitude and to compare with T94 index. Figure 2(a) shows the averaged GHGN of T94 index across the three Δs from $30°$ to $55°$S, as computed at http://www.cpc.nceop.noaa.gov/products/. Figure 2(b) (right) shows our index with the averaged GHGN over mid-latitudes across the three Δ's (from $32.5°$ to $52.5°$S) and the GHGN over mid-high latitudes across one Δ

(from $40°$S to $55°$S). We did not find any new blocking event along the longitude-time grid. Therefore, it does not make sense to show GHGN at low-latitudes. The respective frequency of blocking flows, according to the criterion of Equation (5), is shown at the bottom of each panel of Figure 2. In mid-latitudes, the blocked longitudes in the longitude–time diagram (solid line, Figure 2(b)) seem similar to those shown with the T94 index (Figure 2(a)). However, the frequencies of blocked longitudes at mid-latitudes agree with the blocked longitudes shown in the Hovmöller diagram (Figure 2(b)), whereas the frequency obtained with T94 overestimates the detection as shown in the Hovmöller (Figure 2(a)). In reality, the problem is not the frequency measured with the T94 index, but the fact that the events in the Hovmöller exhibit average values of GHGN around zero between $180°$ and $120°$W, likely due to the presence of stationary blocking events over higher latitudes. We notice that blocking events at high latitudes (Figure 2(b), dotted line) can be observed in Hovmöller diagrams when they are separately computed. For instance, during the winter of 1986 there were two long-living blocking events that lasted for about 17 days (from June 20 to July 8, 1986 - hereafter, e1) and 21 days (from July 24 to August 18, 1986 - hereafter, e2), both appear in Figure 2. The event e1 exhibited a dipole structure at high latitudes with an intense cutoff low equatorward of the blocking ridge (Figure 3(a)). The event e2 exhibited an amplified blocking ridge varying between a dipole and omega blocking types (Figure 3(b)) as indicated by a sequence of synoptic charts (not shown). Both events exhibited similar longitudinal extent of about $40°$. The modified method proposed here seems more efficient in detecting the correct blocking strength as well as the spatial–temporal pattern of blockings.
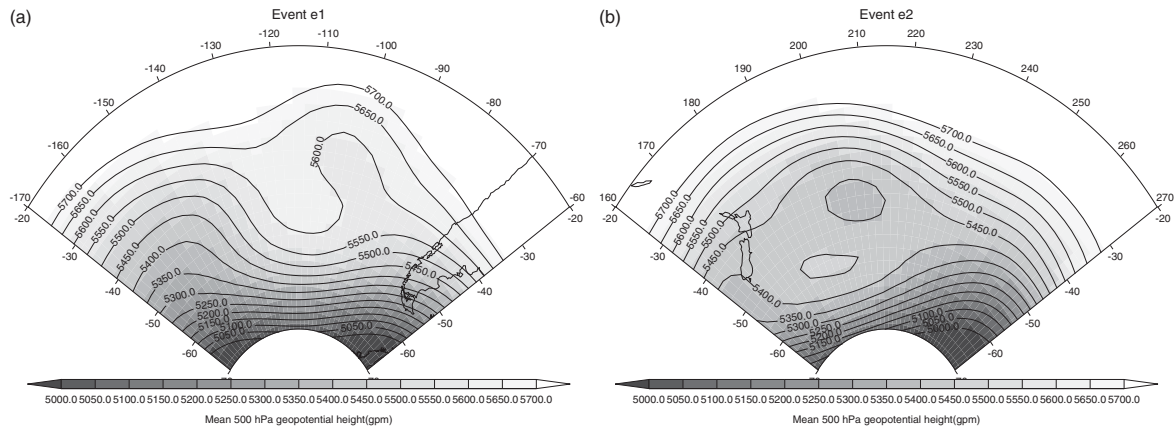
Figure 3. Geopotential height at 500 hPa for (a) the events e1 (20 June–08 July 1986) and (b) e2 (24 July–18 August 1986). Unit: [gpm].

Table III. Classification of ENSO winters according to the Oceanic Niño Index from 1958 to 2010.

El Niño/Southern oscillation						
El Niño			La Niña			
Weak	Moderate	Strong	Weak	Moderate	Strong	Neutral
1969/1976/1977	1958/1963/1965	1972/1982/1997	1962/1983/1995	1964/1970/1971	1973/1988	1959/1960/1961
1992/2004	1986/1987/1991	3 Winters	3 Winters	1974/1975/1984	2 winters	1966/1967/1968
5 winters	1994/2002/2006			1985/1998/1999		1978/1979/1980
	2009			2000/2007/2010		1981/1989/1990
	10 Winters			12 Winters		1993/1996/2001
						2003/2005/2008
	18 Winters			17 Winters		18 Winters

4. Inter-annual variability of blockings and ENSO

To identify ENSO episodes during the SH winter we used the Oceanic Niño Index (ONI)—version 3b of the extended reconstructed sea surface temperature (ERSST) dataset (Smith *et al.*, 2008). Additional information about this dataset can be accessed at http://www.ncdc. noaa.gov/ersst/. This method investigates 3-month running mean of sea surface temperature (SST) anomalies in the Niño 3.4 region (5°N–5°S, 120°–170°W). Moreover, to identify the ENSO phase (El Niño—EN, La Niña—LN or Neutral—NT), we considered a threshold of ±0.5 °C with a minimum of five consecutive overlapping seasons throughout the year. Thus, we considered the occurrence of an ENSO episode during winter when a particular ENSO phase started or was already active during the wintertime and persisted according to the criterion discussed above. The episodes were divided into weak (0.5–0.9 °C), moderate (1.0–1.8 °C), strong (≥1.9 °C) or neutral (when the SST anomaly is between ±0.5 °C). Table III shows the ENSO classification of the winters from 1958 to 2010. According to these criteria, there are 18 winters with NT conditions, 18 winters with EN (divided into: 5 weak, 10 moderate and 3 strong) and 17 winters with LN (divided into: 3 weak, 12 moderate and 2 strong). We classified blocking activity based on the ENSO categories of Table I.

4.1. Timescale for blocking event in the SH

One of the goals of this study is to provide a comprehensive analysis of the long-term climatology of the SH blocking events during the austral winter. To do so, it is important to identify the minimum timescale for blockings in the SH. According to Trenberth and Mo (1985), the relatively stronger westerly winds in the mid and high troposphere of the SH result in shorter duration of blockings in SH comparatively to the NH. Thus, to find the minimum timescale of blocking events we used a method similar to that proposed by Pelly and Hoskins (2003). This timescale can be interpreted as the typical minimum time scale for the weakening of the blocking structure. Thus, a large proportion of events that reached this minimum timescale, may last at least another day.

Figure 4 shows the total number of blocked longitudes lasting at least 1 d plotted on a logarithmic scale base e, during the entire period for a given longitude and at mid to mid-low latitudes and mid to mid-high latitudes. It is noticeable that blocking events tend to persist more over latitudes poleward of the reference latitude (up to 22 days) than over latitudes equatorward of the reference latitude (up to 16 days). A linear regression fit was adjusted and the linear slopes were calculated. The minimum timescale is considered the inverse of the negative slope. These results indicate that blocking events have a minimum timescale of 2.8 days at mid
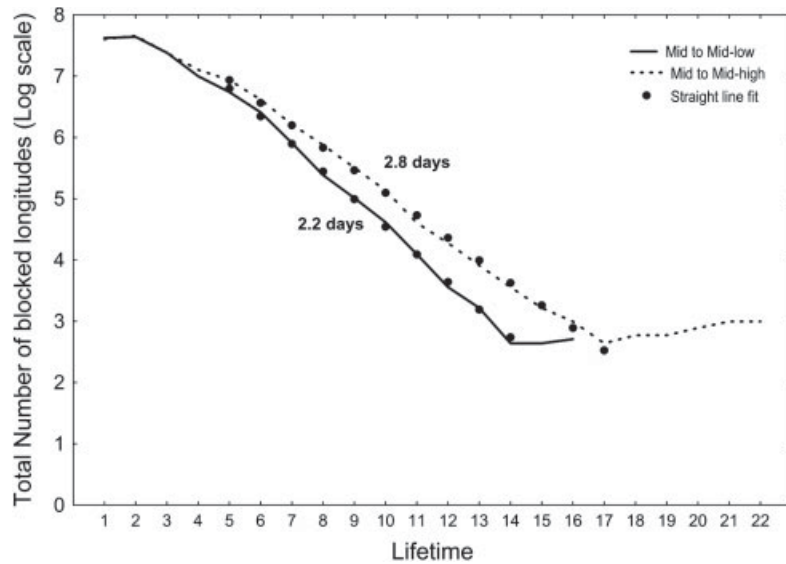
Figure 4. Natural logarithm scale of the total number of contiguous blocked longitudes from 1958 to 2010 during wintertime and lasting at least 1 d over a certain longitude in the mid to mid-low (solid line) and mid to mid-high latitudes (dashed line). Linear regressions are indicated as dot points.

Table IV. Descriptive statistics for identified blocking events for each sector of blocking and throughout the Southern Hemisphere separated according to ENSO categories.

| ENSO condition | Number of winters | West Pacific | | | | | | Central Pacific | | | | | |
| | | Events | | Days | | Lifetime | | Events | | Days | | Lifetime | |
		Total	Avg.	Avg.	Diff.	Avg.	Med.	Total	Avg.	Avg.	Diff.	Avg.	Med.
Weak em	5	*	*	*	*	*	*	*	*	*	*	*	*
Moderate EN	10	34.00	3.40	*16.90*	*−2.71*	4.97	5.00	41.00	4.10	*25.00*	*5.17*	6.10	5.00
Strong em	3	*	*	*	*	*	*	*	*	*	*	*	*
Weak LN	3	*	*	*	*	*	*	*	*	*	*	*	*
Moderate LN	12	42.00	3.50	16.17	−3.44	4.62	4.00	33.00	2.75	*15.00*	*−4.83*	5.45	5.00
Strong LN	2	*	*	*	*	*	*	*	*	*	*	*	*
Neutral	18	75.00	4.17	19.61		4.71	4.00	63.00	3.50	19.83		5.67	5.00

| | | East Pacific | | | | | | Southern Hemisphere | | | | | |
| | | Events | | Days | | Lifetime | | Events | | Days | | Lifetime | |
		Total	Avg.	Avg.	Diff.	Avg.	Med.	Total	Avg.	Avg.	Diff.	Avg.	Med.
Weak em	5	*	*	*	*	*	*	*	*	*	*	*	*
Moderate EN	10	30.00	3.00	*17.20*	*6.64*	*5.73*	*5.00*	122.00	12.20	*66.30*	*10.08*	*5.60*	*5.00*
Strong em	3	*	*	*	*	*	*	*	*	*	*	*	*
Weak LN	3	*	*	*	*	*	*	*	*	*	*	*	*
Moderate LN	12	22.00	1.83	7.92	−2.64	4.32	4.00	123.00	10.25	*47.25*	*−8.97*	4.80	4.00
Strong LN	2	*	*	*	*	*	*	*	*	*	*	*	*
Neutral	18	40.00	2.22	10.56		4.75	4.00	211.00	11.72	56.22		5.04	4.00

The following statistics are displayed: 'number of events' (total—'Tot' and average—'Avg'); 'days with events' (average—'Avg'—and average differences—'Diff') and the 'lifetime of events' (average—'Avg'—and median—'Med'). Underlined values indicate when the differences between EN and LN are statistically significant at *p*-value 0.05 or less. Significant differences from NT winters at *p*-value of 0.05 (0.1) or less are indicated in italics.

to mid-low latitudes and 2.2 days at mid to mid-high latitudes, in accordance with others (e.g. Berrisford *et al.*, 2006). More importantly, these results evidence that the time-scale of blocking events depend strongly on the latitude. Therefore, a minimum timescale of 3 days seems reasonable to represent the mature stage of a blocking event in the SH. Nonetheless, it is important to emphasize that a large proportion of events can last from days up to weeks.

Moreover, we expect atmospheric blocking events to be more persistent than mid-latitudes cyclones. For example, Simmonds and Keay (2000) showed that the average lifetime of mid-latitude cyclones in the SH is about of 2.92 days, but 40% of the cyclones considered in their study lasted less than 2 days. Here, all blocking events lasting at least 3 days have an average lifetime of 4 (5) days at mid to mid-low (high) latitudes (see Table IV).
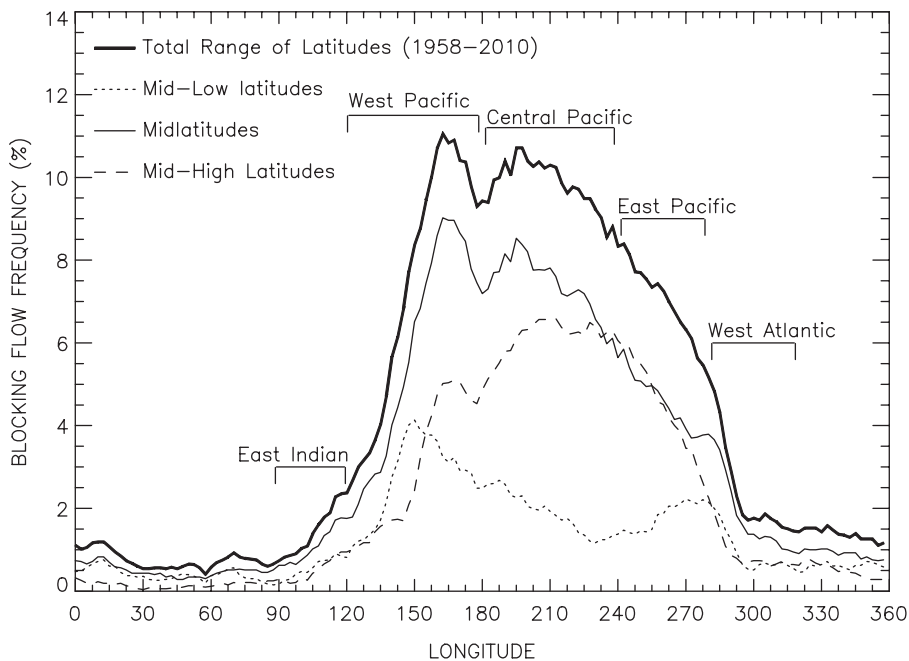
Figure 5. Frequency of blocked longitudes separated according to the mid-low, mid-, mid-high latitudes and for the total range of the latitudes during NT winter. Dotted line shows mid-low latitudes. Dashed line shows mid-latitudes. Dot-dashed line shows mid-high latitudes and thick solid line shows the total range.

4.2. Characteristics of winter blocking events

On the basis of 53 austral winters, we found a total of 3268 days with blocked longitudes and 584 blocking events lasting at least 3 days, an average of 9.9 events per winter. About 211 of these events were detected during NT winters, 210 during EN winters and 163 during LN winters. Also, about 13% (7%) of these days occurred simultaneously over WPA and EPA (EIN and CPA). Figure 5 displays the frequency of blocked longitudes distributed along the longitudes and according to the reference latitudes of the blocking index during the whole period, and separated by zonal bands. The total range of latitudes (Figure 5, bold lines) suggests that a maximum frequency was observed in a narrow region between 140°E and 180°, named here as WPA sector. In this sector, the SH blockings were detected primarily over mid-latitudes (32.5°S to 52.5°S) (Figure 5, solid thin-lines). Following this, an extensive area with similar frequency was located between 180° and 120°E, named here as CPA. The sum of these two regions was named by T94 as the Australian-New Zealand region. However, according to Figure 5, it seems obvious that SH blockings may occur well beyond New Zealand over the Central Pacific. There is a third region between 120°E and 80°E detected for the first time by Rutllant and Fuenzalida (1991) and later confirmed by Sinclair (1996), where blocking events are distinguished by their predominant location over mid-high latitudes (40°S to 55°S) (Figure 5, dashed lines). Other regions, such as East Indian and West Atlantic Ocean will not be discussed in detail, because they represent events that are not significant at *p*-value of 0.05 or less. The high frequency of blocking events at mid-high latitudes eastward of 150°E seems related to

the propagation of large-scale wave trains from Australia to high latitudes and around Southern South America following a typical arc-like route that has been largely documented (e.g. Karoly, 1989; Ambrizzi *et al.*, 1995; Renwick and Revell, 1999; Nascimento and Ambrizzi, 2002).

Additionally, all events lasting at least 3 days had a median (average) lifetime of about 5 (5.7) days over the CPA sector, whereas a median (average) of about 4 (4.7) days was found over WPA and EPA sectors. This result is consistent with Sinclair (1996), who analysed a short period of 10 years and used a different criterion to identify blocking events (lasting at least 2 days) and found an annual average lifetime of about 5 days.

4.3. Blocking activity during ENSO phases

To examine changes in the blocking events according to ENSO variability we compared the frequency of blocked longitudes during opposite ENSO phases against NT conditions. To assess the statistical significance for the difference in frequency, location, number of events and duration, a *z*-score two-tail test was used. Differences were considered significant at $p \leq 0.05$ and ≤ 0.10 significance levels. The *z*-score was defined by Equations (6 and 7):

$$z\,(\lambda) = 2.\left\{\frac{(p_{w/c} - p_n)}{\mathrm{SE}}\right\} \qquad (6)$$

The *z*-score of Equation (6) was computed for each 'longitude point', where, $p_{w/c}$ is the proportion of blocked longitudes for EN (*w*) or LN (*c*) winters, p_n is the proportion of blocked longitudes for NT winters and SE
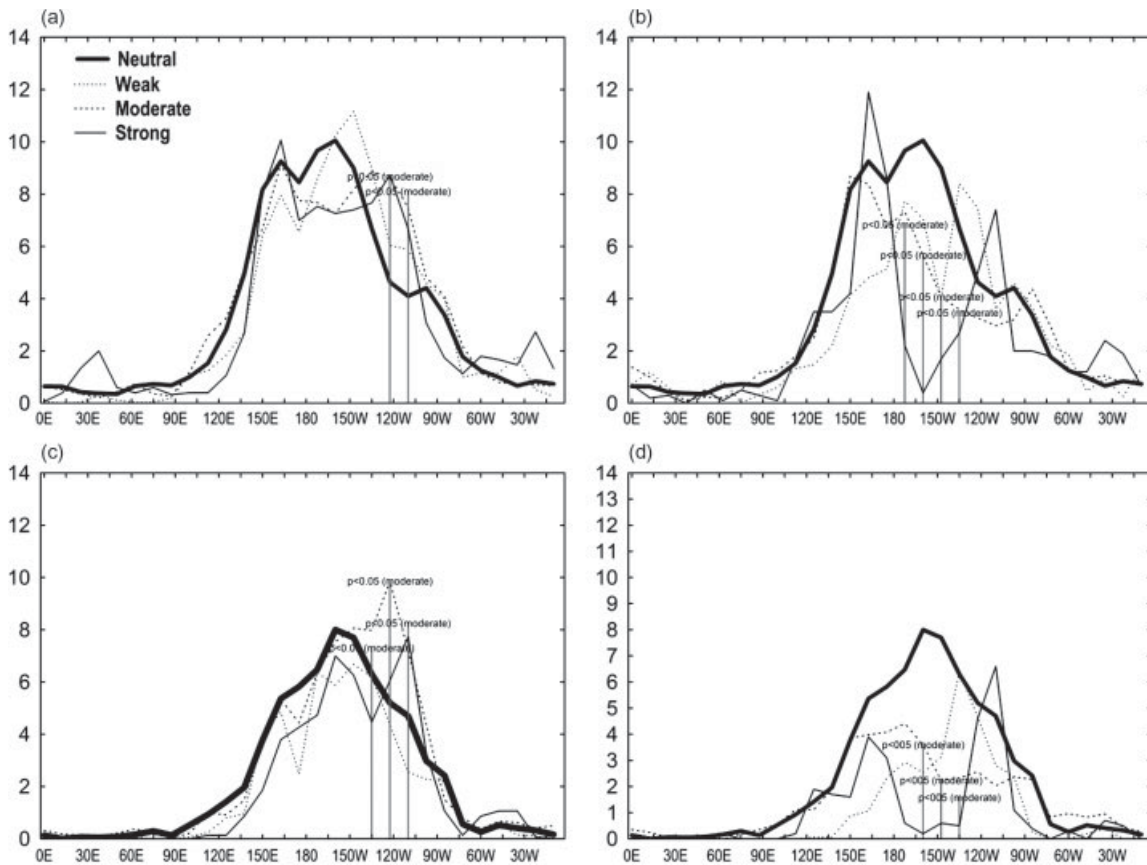
Figure 6. Frequency of blocked longitudes during wintertime according to weak (dotted line), moderate (dashed line) and strong (solid line) categories of ENSO at mid-latitudes (upper row) and mid-high latitudes (bottom row), respectively. EN and LN winters are shown in the left and right columns, respectively. NT winters are shown as black thick-lines with one standard deviation (grey bars) for comparison.

is the standard error. All proportions are expressed in percentage and computed for each longitude point.

$$z = 2.\left\{ \frac{(N_n.N_{w/c})}{N_n + N_{w/c}} \cdot (R_n - R_{w/c}) \right\}. \qquad (7)$$

The z-score of Equation (7) was computed for each 'sector of blocking', where $N_n(N_{w/c})$ is the total number of blocking events during NT (EN or LN) winters; $R_n(R_{w/c})$ is the proportion p/p', where p is the total number of blocking events above the common median and p' is the total number of blocking events during NT (EN or LN) winters. The common median is defined as the median obtained by combining NT with EN/LN winters.

Figure 6 displays the blocked longitudes at mid-latitudes (Figure 7, upper row) and mid-high latitudes (Figure 7, bottom row), respectively, during the SH winter separated according to weak (dotted line), moderate (dashed line) and strong (solid thin-line) category of ENSO winters. EN and LN winters are shown in the left and right columns, respectively. NT winters are shown as black thick-lines for comparison with each other. Grey thin-bars indicate the significant longitudinal extent at p-value of 0.05 or less.

As shown in Figure 6 (left column), large differences in the frequency and preferred locations of blocked longitudes exist among ENSO categories. For instance,

weak EN shows a relative increase (decrease) in mid-latitudes for blocked longitudes in relation to NT over the CPA (WPA) sector (Figure 6(a)), but the frequency is similar to the NT winters over mid-high latitudes (Figure 6(c)). However, during moderate to strong EN winters, and in particular during moderate EN, there is no increase in frequency at mid-latitudes; however, blocking frequency over mid-high latitudes shifted eastward over $120°$W (Figure 6(c); $p < 0.05$) indicating a preference for high-latitude blockings.

On the other hand, a significant decrease ($p < 0.05$) (Figure 6, right column) in the frequency of blocked longitudes was observed across de entire CPA sector (Figure 6(b)), mainly at mid-high latitudes (Figure 6(d)) and during all categories of LN winters (only moderate LN winters are statistically significant). This can be due to the dynamical interactions between ENSO and SAM and is discussed in Section 6. Interestingly, weak and strong LN, although not statistically significant, show similar enhanced frequency over the EPA sector, compared with those found during moderate to strong EN categories. However, the small sample size of these extreme categories limits the statistical significance of these results.

Figure 7 shows blocked longitudes detected considering the total range of latitudes (upper panel) during EN
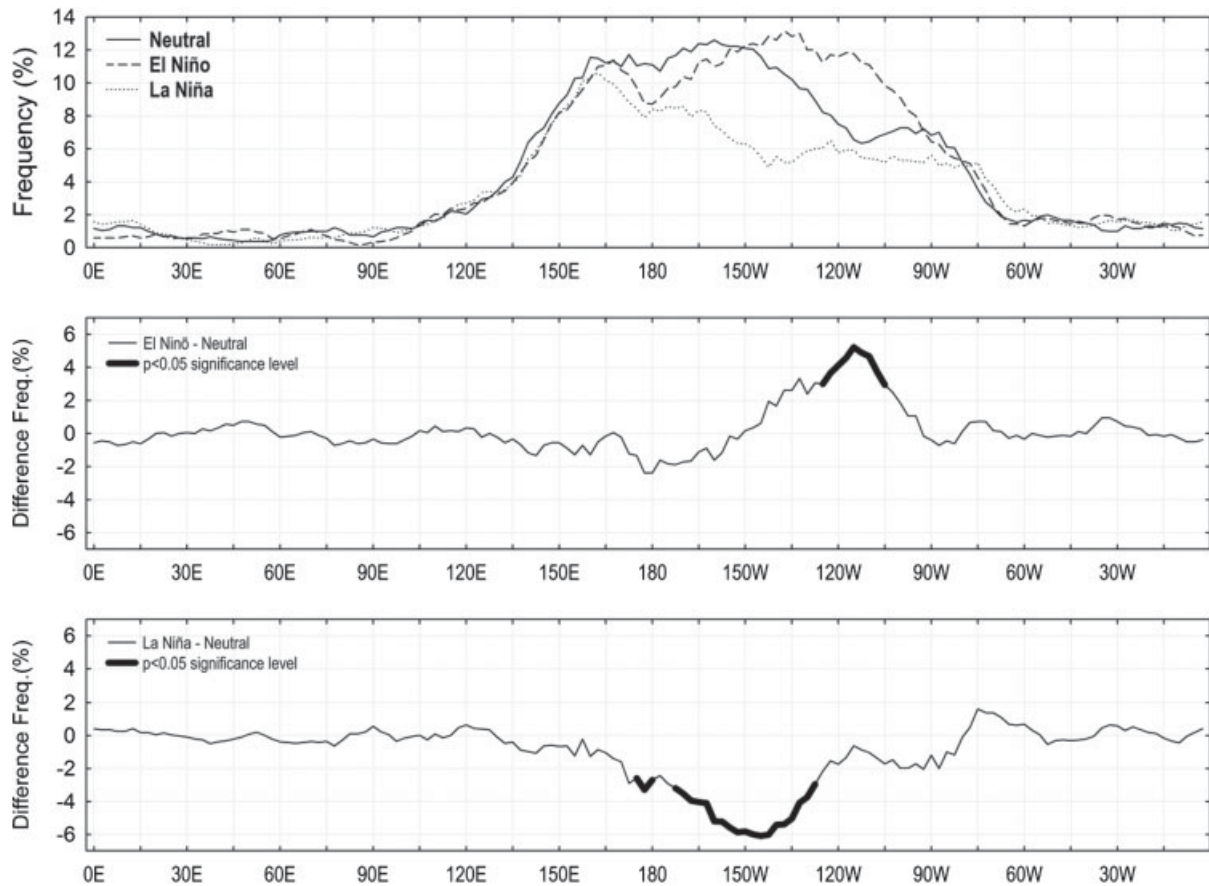
Figure 7. Frequency of blocked longitudes detected on the total range of latitudes (upper panel) during EN (dashed line) and LN (dotted line) winters without taking into account the categories of ENSO. NT winters are shown as a solid line. Frequency differences relatively to NT winters are shown for EN (middle) and LN (bottom) with z-score two-tailed tests at p-value of 0.05 or less (bold lines).

(dashed line) and LN (dotted line) winters without taking into account ENSO categories. NT winters are shown as a solid line. Frequency differences in relation to NT winters are shown in the Figure 7 for EN (Figure 7, middle) and for LN (Figure 7, bottom) with z-score two-tailed test at $p < 0.05$ (bold lines) according to Equation (5). As previously discussed, the EN phenomenon changes the preferred locations of blocked longitudes towards the EPA sectors (Figure 7, middle panel—bold line) in accordance with others (e.g. Renwick 1998). On the other hand, the LN phenomenon suppresses blocked longitudes over the eastern portion of the WPA sector and across the entire CPA sectors (Figure 7, bottom panel—bold line). These results cannot be properly compared with Renwick (1998), because the author has compared EN years against non-EN years (NT + LN). Here, we showed that the frequency of SH blockings during NT winters are statistically different from LN winters across the South Pacific, except over the EPA sector (Figure 7).

Table IV provides additional information on the statistical properties of blockings, focusing on events lasting 3 days or more over the South Pacific during wintertime. The following properties of SH blockings are shown: 'number of events' expressed as total and average; 'days with events' in terms of average and average differences and the 'lifetime of events' in terms of average and

median. EIN and WAT sectors were not shown because they are not significant at p-value of 0.05 or less. The observed values for the NT winters are shown at the bottom of the table for comparison with the opposite ENSO phases. Significant differences from NT winters at p-value of 0.05 (0.1) or less are indicated in italics. Also, 'underlined' values indicate when the differences between EN and LN are statistically significant at p-value 0.05 or less. Weak and strong categories are not shown.

The results of Table IV confirm that during moderate EN winters there is a significant ($p \leq 0.05$) enhancement in the number of days with blocking events over the eastern portion of the CPA and EPA. This result is consistent with Rutllant and Fuenzalida (1991) and Renwick (1998), regardless of their methodologies. However, differently from other authors (e.g. Renwick, 1998; Marques and Rao, 2000; Wiedenmann *et al.*, 2002), we find significant differences during winter. In addition, it is also observed during moderate EN a slightly statistically significant suppression over WPA in accordance to Renwick (1998). Regarding blocking lifetime, there is indication that blocking events in the EPA sector during moderate EN winters increases in about 1 d ($p < 0.05$) the median lifetime in relation to both NT and LN winters, suggesting more extreme events over this sector. This is likely due to an increase in high-latitude
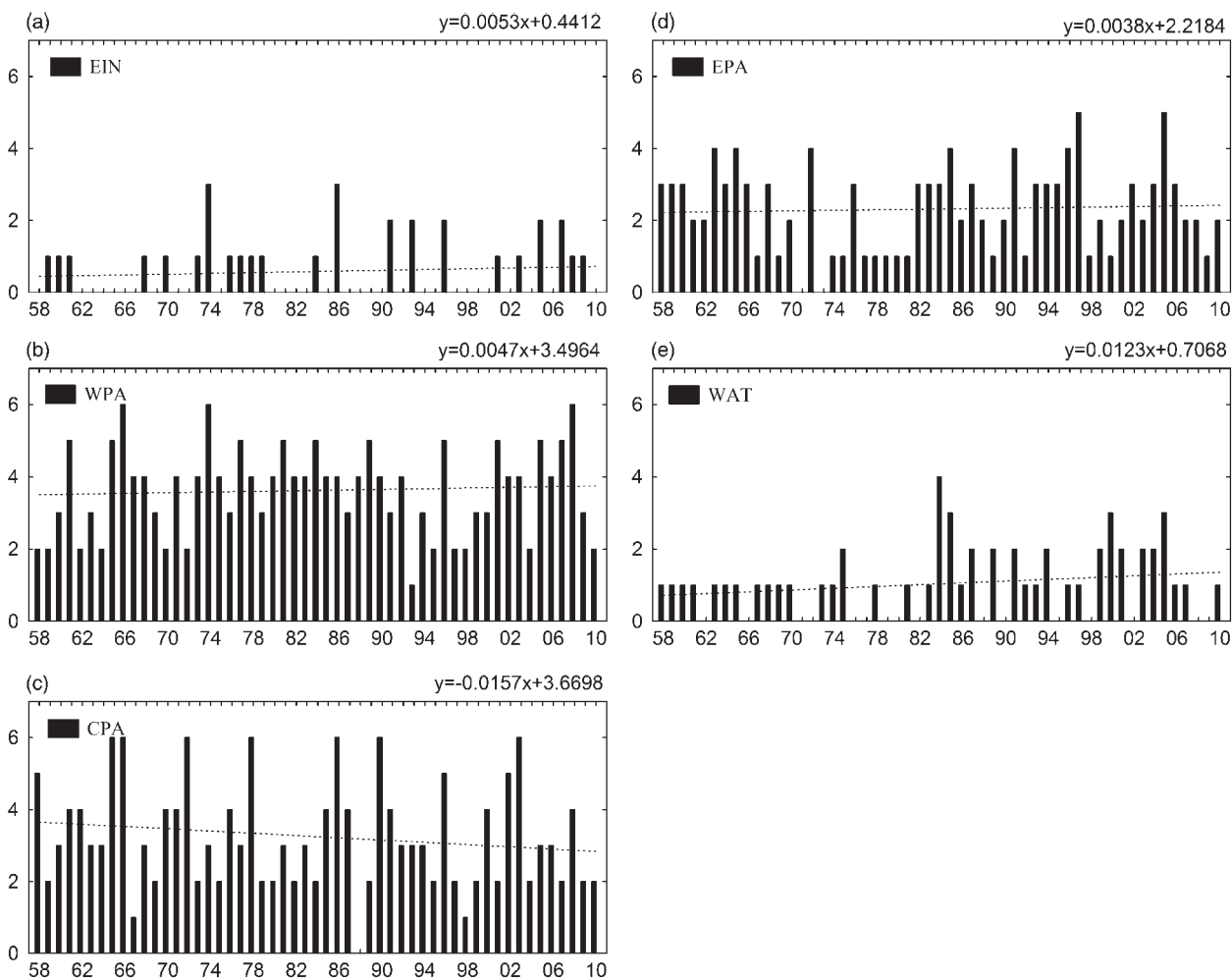
Figure 8. Statistical distribution of number of blocking events during wintertime over the East Indian (a), West Pacific (b), Central Pacific (c), East Pacific (d) and West Atlantic oceans (e). Linear trends are indicated (dotted line).

blockings over the EPA sector. On the other hand, during moderate LN winter, the total number of days of a blocking event significantly decreases across the SH, which is more evident over the entire CPA sector. Moreover, we found no significant differences in the number of blocking events in relation to NT winter climatology. These results show only a significant ($p \leq 0.05$) large variability in the number of days with blocking events across the South Pacific sectors, also between the opposite moderate ENSO phases (underlined).

Finally, in previous studies, the blocking activities in the South Pacific regions during opposite ENSO phases were not properly compared with NT winters. Here, we show that NT winters are statistically different from opposite ENSO phases. In general, our results show a good agreement with others (e.g. Rutllant and Fuenzalida, 1991; Sinclair, 1996; Renwick, 1998; Marques and Rao, 2000; Wiedenmann *et al.*, 2002), except that this study provides much more information about the statistical properties of SH blocking events during wintertime. In Section 6, we will discuss the joint influence of ENSO and SAM on the variability of the number of days with blocking events.

5. Trends in blockings

This section investigates trends in blocking events from 1958 to 2010 defined according to the criteria discussed in Section 2. Figure 8 shows the distribution of number of blocking events during the winter over East Indian (a), West Pacific (b), Central Pacific (c), East Pacific (d) and West Atlantic oceans. Linear trends are indicated in the figures. The significance of trends was tested following the method discussed in Jones and Carvalho (2006). The test was performed by shuffling the frequency of blocking events and fitting a linear trend 2500 times. The actual angular coefficient was compared with the 95th percentile of the frequency distribution of the 2500 angular coefficients obtained from the randomization. A slightly positive (negative) trend in SH blocking events was observed in EIN, WPA and EPA (CPA) sectors. However, based on the statistical test all trends were not significant at $p \leq 0.05$. Nevertheless, we observe a large interannual variability in the number of events. Figure 9 shows the total number of blocking events (defined according to Section 2) and the respective 11-year running variance. The linear trend is not statistically significant at $p \leq 0.05$ level (not shown). On
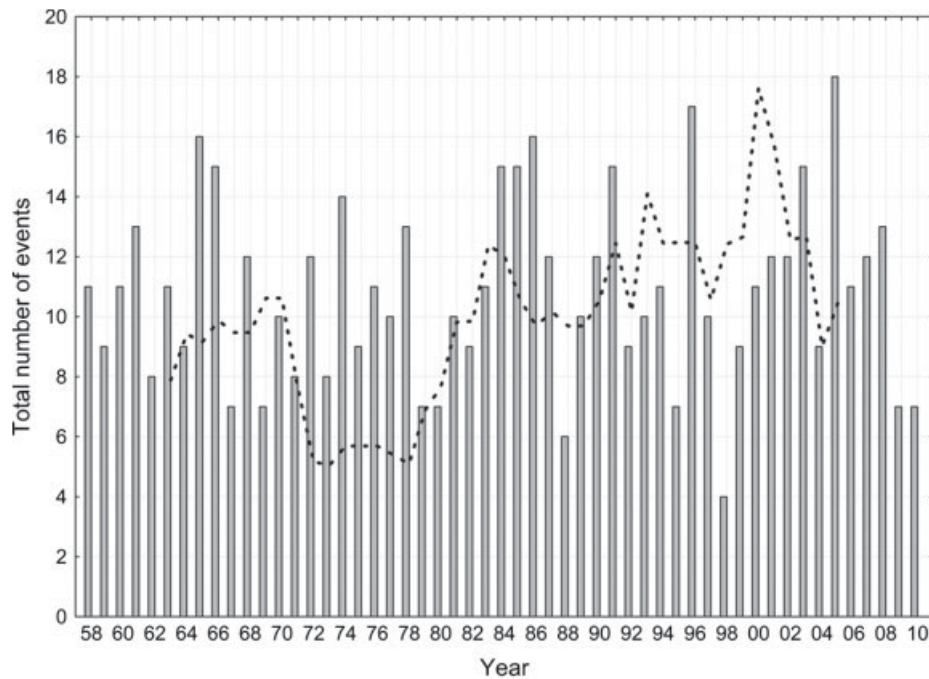
Figure 9. Total number of the SH blocking events in the wintertime from 1958 to 2010. Bars are total number of blocking events per year. Dotted line is the running 11-year variance, plotted at the mid-point of 11-years period.

the other hand, the running variance indicates the existence of decadal variability in the number of events, possibly related to decadal changes in the Pacific SST (Deser *et al.*, 1996; Guilderson and Schrag, 1998).

6. Combined effect of ENSO and SAM phases on the variability of the SH blocking events

To explore the effect of ENSO and SAM phases on the variability of blocking events, we investigated the spatial patterns of the upper troposphere circulation from 1982 to 1999, as well as the main statistical properties of blocking events. The period was conveniently chosen because the number of El Niño equals the number of La Niña events (seven events in each ENSO phase). The daily SAM index was obtained from the Climate Prediction Center (CPC) National Center for Environmental Prediction (NCEP) (online at http://www.cpc.ncep.noaa.gov). It was calculated by projecting the 700-hPa geopotential height anomaly onto the leading mode (EOF-1) derived from monthly mean 700-hPa height anomalies from 20° to 90°S. The time series were normalized by the standard deviation of the monthly index (1979–2000 base period). Positive SAM (SAM+) and negative SAM (SAM−) phases of the index were defined when the magnitude of the daily SAM anomalies exceeded one (or was below minus one) standard deviation. The combined influence of SAM and ENSO phases upon the blocking activities was characterized according to four combinations of the indices as follows: (a) SAM−|LN; (b) SAM−|EN; (c) SAM+|LN and (d) SAM+|EN. During 1982–1999 there were 7 years with EN phase and 7 years with LN phase.

Table V. Descriptive statistics of the effect of the combined phases of ENSO and SAM modes.

	SAM−				SAM+			
	ND	NB	N3d	MLF	ND	NB	N3d	MLF
ENSO+	131	83	54	13	67	39	30	6
ENSO−	103	56	45	8	142	67	35	3

The following statistics are displayed, total number of days for each combined phases (ND), total number of days with blocked longitudes (NB), total number of days with blocking event lasting at least 3 days (N3d), and maximum lifetime of the blocking events (MLF).

Table V shows the total number of days for each combined phases of ENSO and SAM, the total number of days with blocked longitudes, the total number of days with blocking event lasting at least 3 days, and maximum lifetime of the blocking events, respectively. There are no statistically significant differences in the number of days with SAM− between the opposite ENSO phases at $p \leq 0.1$, whereas the number of days with SAM+|LN is twice the number observed during SAM+|EN and this difference is significant at $p \leq 0.05$ confidence level. Moreover, Table V also suggests that the number of days in a blocking event during SAM− is larger for both ENSO phases. The high frequency of days with SAM+ during LN winter might be the reason for the significant decrease in the number of days with blocking events. Other important result in Table V is the increase in the maximum life time duration of the blocking events during the SAM−|EN compared with SAM−|LN (13 and 8 days, respectively). During the SAM+ the blocking events are less persistent in both ENSO phases
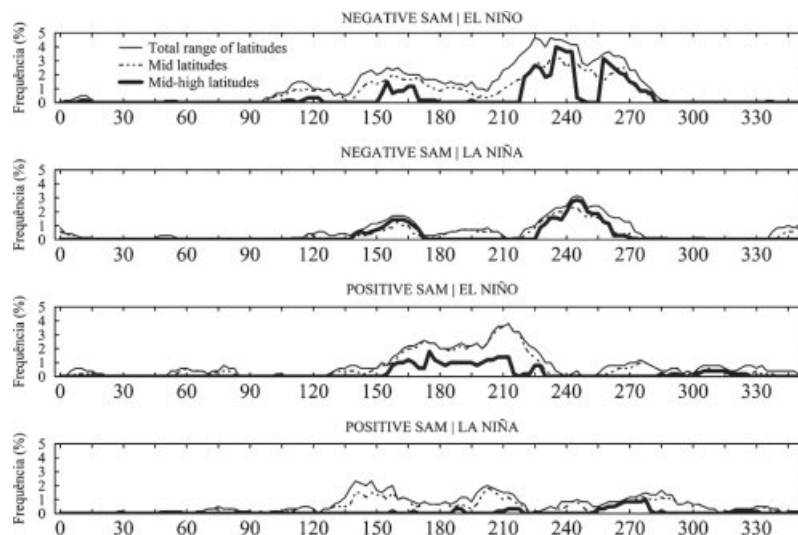
Figure 10. Frequency (%) of blocked longitudes according to SAM|ENSO combinations: top row: SAM−|EL NIÑO; second middle row: SAM−|LA NIÑA; third middle row: SAM+|EL NIÑO; bottom: SAM+|LA NIÑA. Black thin lines indicate the 'Total range' of latitudes; Black dashed lines indicate 'mid-latitudes' and black thick lines are 'mid-high' latitudes.

comparatively to SAM−. However, the ratio between the maximum blocking duration in the opposite ENSO phases, that is SAM + |EN and SAM + |LN conditions (6 and 3 days, respectively), seems to hold.

Figure 10 shows the frequency of blocked longitudes separated according to the reference latitudes at mid (shaded line) and mid-high latitudes (solid bold-line), including the total range of latitudes (solid thin-line) as previously defined and for all SAM|ENSO combinations. Considering that the typical lifetime of SH blocking events at mid-high is slightly longer (about of 0.5 days event^{-1}) than over mid-latitudes (Figure 4), some interesting aspects can be extracted from Figure 10. The preferred locations for blocking events during SAM− occur at mid-high latitudes (bold lines) over the EPA sectors for both ENSO phases, whereas the frequency SH blocked longitudes over the western portion of the CPA sector decreases. These differences are significant at $p \leq 0.05$ during EN conditions (see Figure 7). During SAM + |EN the preferred locations for SH blockings seem to occur over the WPA and western portion of the CPA sectors. During SAM + |LN we observe a lower frequency throughout the SH. However, some increase is observed over West Atlantic region during SAM + |LN. The variability of SAM is largely related to ENSO (e.g. Carvalho *et al.*, 2005), and these interactions control the frequency and preferred locations of SH blocking events.

These results indicate that the high frequency of SAM + during LN winters plays a major role for the significant suppression in the number of days with blocking event between WPA and the western portion of the CPA sector (Figure 7). Thus, we investigate in detail why SAM + |LN inhibit blocking event formation over the South Pacific Basin. Trenberth (1986) showed that transient eddies accelerate the westerlies in the main storm track and to the south of a blocking anticyclone, but they act to decelerate the westerlies near the main split in

the jet and thus help to maintain the blocking. Since the GHGN provides a measure of zonal flow intensity, the presence of easterly anomalies between 35°S and 50°S is important to detect contiguous blocked longitudes. Chen and van den Dool (1997a) emphasized that the poleward location of the jets favours a high frequency of blocking events. According to Lejenäs (1984), the presence of easterly anomalies at these latitudes indicates the blocking events position. Thus, the strengthening of the polar jet around the latitude of 60°S creates unfavourable conditions for formation of blocking events due to the strengthening of the westerlies. On the other hand the strengthening of the subtropical jet is clearly important for the maintenance of blocking events due to its association with the jet split.

To exemplify the relationships discussed above, we have separated 'zonal regimes' from 'blocking regimes'. A blocking regime means the presence of blocked longitudes during a blocking event with strong meridional deformation. On the other hand, a zonal regime means no blocking presence. Thus, Figure 11 shows composites of zonal wind anomalies at 200 hPa (annual cycle removed) during 'zonal' and 'blocking regimes' and according to SAM|ENSO combinations, and highlights some important mechanisms explaining unfavourable and favourable conditions for blocking.

For instance, the zonal regimes (Figure 11—on the left), indicates the strengthening of the polar jet in the latitude around 60°S and the absence of the subtropical jet during SAM + for both ENSO phases. As mentioned before, these features are unfavourable for blocking formations because the westerlies accelerate over mid-latitudes. On the other hand, during SAM− , for both ENSO phases, the polar jet is confined near the pole and the subtropical jet is strengthened with the presence of the easterly anomalies between the two jets (around latitudes of 60°S), creating favourable condition for the bifurcation

Zonal Regime SAM-|EL NINO

Blocking Regime SAM-|EL NINO

Zonal Regime SAM-|LA NINA

Blocking Regime SAM-|LA NINA

Zonal Regime SAM+|EL NINO

Blocking Regime SAM+|EL NINO

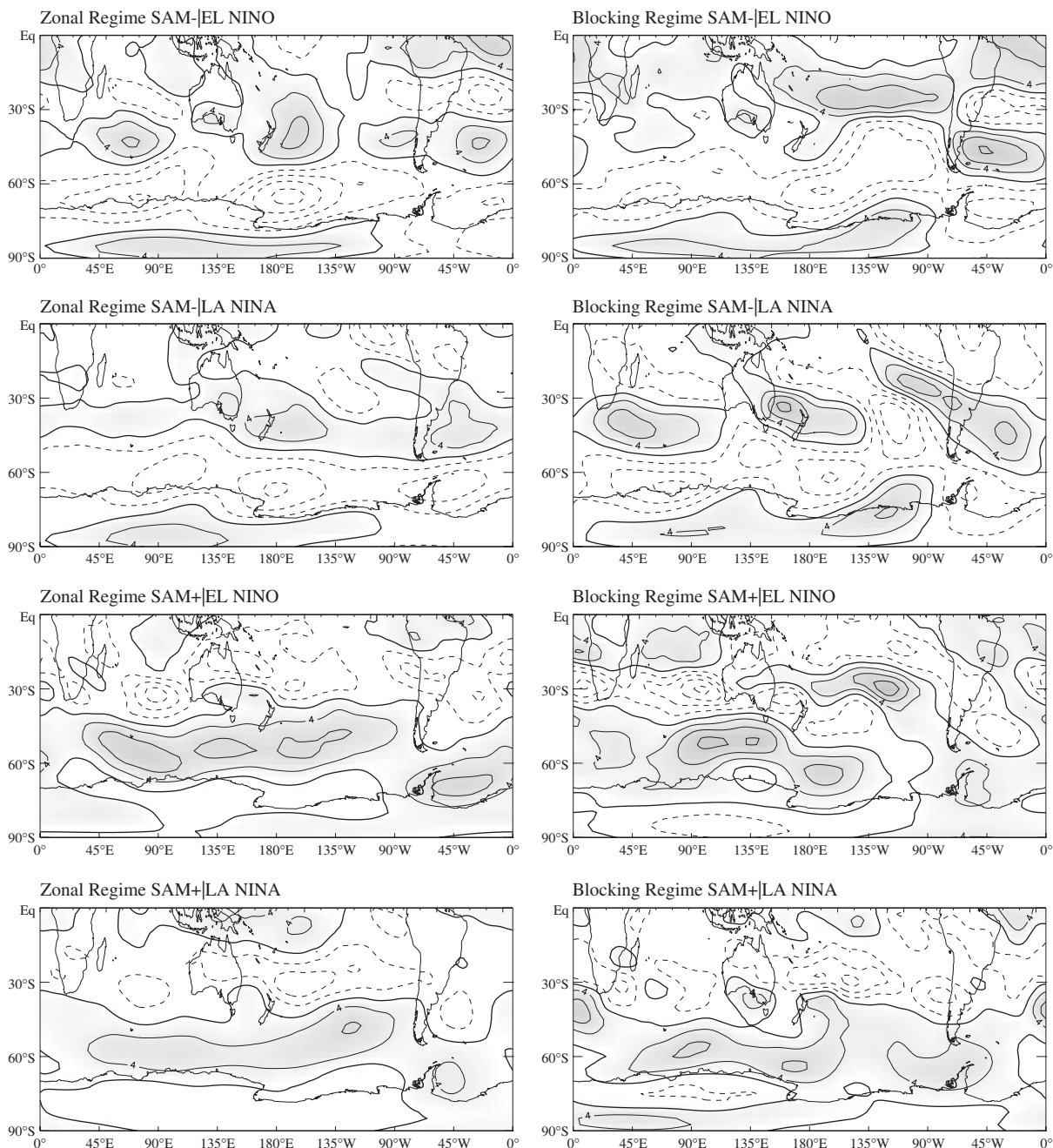Zonal Regime SAM+|LA NINA

Blocking Regime SAM+|LA NINA

Figure 11. Composites of 200 hPa zonal wind anomalies for SAM|ENSO combinations during Zonal (left column) and Blocking Regimes (right column): from top to bottom: SAM−|EL NIÑO, SAM−|LA NIÑA, SAM+|EL NIÑO and SAM+| LA NIÑA. Grey regions indicate the positive anomalies with statistical significance at 95% level of confidence. Units: $(m\,s^{-1})$.

zones and blocking formation. The jet locations and intensities during different SAM phases are in good agreement with the results obtained by Carvalho *et al.* (2005). In contrast, the blocking regimes for SAM−|EN (Figure 11—on the right) indicate the presence of easterly anomalies in the latitudes between 35°S and 50°S and from 150°W to 80°W due to the strong deformation in the zonal flow. These features suggest high frequency of blocking events in the eastern portion of the CPA and in the EPA sectors. In this situation, the polar jet stays near the poles and the subtropical jet is strengthened in the South Pacific Ocean. A similar

configuration of the zonal circulation is observed during SAM−|LN; however, a break in the subtropical jet over the CPA sector occurs near the longitude of 135°W. On the other hand, during SAM + |EN we observe the presence of easterly anomalies over a narrow latitudinal range extending from Southeastern Australia toward New Zealand, indicating the preferred locations for blocking events from 150°E to 135°W. In contrast to the other three combinations, the SAM + |LN is associated with the least favourable conditions for blocking events to occur due to the strengthening of the polar jet around the latitude of 60°S and the non-existence of a significant

subtropical jet. This explains the significant suppressed number of days with SH blocking over the WPA and the western portion of the CPA sector. Among the main reasons for the difference between SAM + |EN and SAM + |LN is that the EN phenomenon modulates the subtropical jet such that favourable conditions for blocking events are more likely to occur than during LN events.

A relevant question to be answered is whether the observed preference for blockings changes according to opposite SAM phases. A statistical test (at 5% significance level) for the difference in proportion of SH blocking events in each sector and for opposite SAM phases was carried out. The results show that the proportion of blockings increases over the East Indian and all Pacific sectors during SAM− compared to SAM+ in both ENSO phases. On the other hand, the test shows that there is an increase in the frequency of SH blockings over West Atlantic during SAM+. When we compare SAM−|EN with SAM−|LN, no significant difference was found. However, there are more blocking events during SAM + |EN than during SAM + |LN.

7. Summary and conclusions

This observational study describes 53-years wintertime climatology of blocking in the SH using NCEP/NCAR reanalysis. We provide a comprehensive analysis of the main statistical properties and preferred locations of blockings stratified according to categories of the ENSO cycle and we investigate the combined effects of ENSO and SAM phases on blocking frequency. To improve the identification of spatial variations of blocking events throughout the SH, conventional indices are revised and adapted to a higher spatial resolution and were applied to detect blocking events in three latitude bands.

We find that a timescale of 3 days (rather than 5 days) is more appropriate for a mature blocking event in the SH due to the strong westerly winds in the troposphere of the SH. Also, we show that SH blocking events are more persistent at high latitudes, consistent with other studies.

Opposite phases of the ENSO cycle are classified into three categories, weak, moderate and strong and were compared against ENSO-Neutral according to Oceanic Niño Index conditions at p-value of 0.05 or less. The results show that the SH blocking events exhibit different behaviours depending on ENSO category. For instance, during moderate EN winters the blocking frequency is significantly enhanced over higher latitudes and shifted eastward over $120°W$, which is consistent with other studies. Also, there is an increase (decrease) of the number of days associated with blocking events over CPA and EPA (WPA). However, there is no statistically significant change in the total number of events in the SH. There is indication that during EN there are many more extreme events over the EPA sector, and the median duration of these events increases in one day. On the

other hand, moderate LN is characterized by a significant decrease of the total number of days associated with a blocking event across the SH, with larger impact over the CPA sector. Also, there are no statistically significant impacts in the total number of events during LN winters

A positive (negative) trend in SH blocking events is observed for EIN, WPA and EPA (CPA) sectors; however, none of these trends are statistically significant at p-value of 0.05 or less. This result agrees with Wiedenmann *et al.* (2002). The analysis of 11-year running variance indicates the existence of a decadal change in the variability of blocking events, possibly related to decadal changes in the Pacific SST (Deser *et al.*, 1996; Guilderson and Schrag, 1998).

The combined effect of ENSO and SAM modes significantly impacts the frequency and the preferred locations of blockings. SAM− combined with EN plays a major role for the enhanced number of days with blocking events over the eastern portion of the CPA and EPA sectors. On the other hand, atmospheric conditions associated with SAM+ along with LN are unfavourable for the formation of blockings due to the strengthening of the polar jet around the latitude of $60°S$, which plays a significant role for the decreased number of days with blocking events across the South Pacific, with larger impact in the WPA and the western portion of the CPA sectors. On the other hand, SAM+ combined with EN winters create favourable conditions for the formation of blocking events over WPA and the western portion of the CPA sectors due the modulation of the subtropical jet by EN. These results show that the variability of SAM combined with ENSO plays a major role for preferred locations and frequencies of SH blocking events. This study points out the importance of monitoring and forecasting tropical–extratropical interactions on a broad range of temporal and spatial scales to properly understand, forecast and predict variations and changes in blockings and their implications for weather patterns in the SH.

References

Ambrizzi T, Hoskins BJ, Hsu H-H. 1995. Rossby wave propagation and teleconnection patterns in the Austral Winter. *Journal of the Atmospheric Sciences* **52**: 3661–3672.

Barriopedro D, Garcia-Herrera R, Lupo AR, Hernández E. 2006. A climatology of Northern Hemisphere blocking. *Journal of Climate* **19**: 1042–1063.

Barry RG, Chorley RJ. 1992. *Atmosphere, Weather and Climate*, 6th edn. Routledge: London; 392.

Berrisford P, Hoskins BJ, Tyrlis E. 2006. Blocking and Rossby wave breaking on the Dynamical Tropopause in the Southern Hemisphere. *Journal of the Atmospheric Sciences* **64**: 2881–2898.

Blackmon ML, Mullen SL, Bates GT. 1986. The climatology of blocking events in a perpetual simulation of a spectral general circulation model. *Journal of the Atmospheric Sciences* **43**: 1379–1405.

Carvalho LMV, Jones C, Ambrizzi T. 2005. Opposite phases of the Antarctic Oscillation and relationships with intraseasonal to interannual activity in the Tropics during the Austral Summer. *Journal of Climate* **18**: 702–718.

Carvalho LMV, Jones C, Silva AE, Liebmann B, Silva Dias PL. 2011. The South American Monsoon System and the 1970s climate transition. *International Journal of Climatology* **31**: 1248–1256. DOI: 10.1002/joc.2147

Casarin DP. 1983. Um estudo observacional sobre os sistemas de bloqueio no hemisfério sul. São José dos Campos. In *Dissertação (Mestrado em Meteorologia)*. Instituto Nacional de Pesquisas Espaciais, INPE-2638-TDL/114, 82 pp (in Portuguese).

Charney JG, Shukla J, Mo KC. 1981. Comparison of a barotropic blocking theory with observation. *Journal of the Atmospheric Sciences* **38**: 762–779.

Chen WY, van den Dool HM. 1997. Asymmetric impact of tropical SST anomalies on atmospheric internal variability over the North Pacific. *Journal of the Atmospheric Sciences* **54**: 725–740.

Colucci SJ, Alberta TL. 1996. Planetary-scale climatology of explosive cyclogenesis and blocking. *Monthly Weather Review* **124**: 2509–2520.

Damião MCM, Trigo RM, Cavalcanti FAI, DaCamara CC. 2008. Blocking episodes in the southern hemisphere: impact on the climate of adjacent continental areas. *Pure and Applied Geophysics* **165**: 1941–1962. DOI: 10.1007/s00024-008-0409-4.

Deser C, Alexander MA, Timlin MS. 1996. Upper ocean thermal variations in the North Pacific during 1970–1991. *Journal of Climate* **9**: 1840–1855.

Dole RM. 1986. The life cycles of persistent anomalies and blocking over North Pacific. *Advances in Geophysics* **29**: 31–69.

Dole RM, Gordon ND. 1983. Persistent anomalies of the extratropical Northern Hemisphere wintertime circulation: geographical distribution and regional persistence characteristics. *Monthly Weather Review* **111**: 1567–1586.

Elliott RD, Smith TB. 1949. A study of the effects of large blocking highs on the general circulation in the northern-hemisphere westerlies. *Journal of Meteorology* **6**(2): 67–85. ISSN 0095–9634.

Fogt RL, Bromwich D, Hines KM. 2010. Understanding the SAM influence on the South Pacific ENSO teleconnection. *Climate Dynamics*. DOI: 10.1007/s00382-010-0905-0.

Frederiksen JS. 1982. A unified three-dimensional instability theory of the onset of blocking and cyclogenesis. *Journal of the Atmospheric Sciences* **39**: 969–982.

Gong D, Wang S. 1999. Definition of Antarctic Oscillation index. *Geophysical Research Letters* **26**: 459–462.

Guilderson TP, Schrag DP. 1998. Abrupt shift in subsurface temperatures in the tropical Pacific associated with changes in El Niño. *Science* **281**: 240–243.

Hartmann DL, Lo F. 1988. Wave-driven zonal flow vacillation in the southern hemisphere. *Journal of the Atmospheric Sciences* **55**: 1303–1315.

Hines KM, Bromwich DH, Marshall GJ. 2000. Artificial surface pressure trends in the NCEP-NVAR reanalysis over the southern ocean Antarctica. *Journal of Climate* **13**: 3940–3952.

Hoskins BJ, McIntyre ME, Robertson AW. 1985. On the use and significance of isentropic potential vorticity maps. *The Quarterly Journal of the Royal Meteorological Society* **111**: 877–946.

Jones C, Carvalho LMV. 2006. Changes in the activity of the Madden-Julian oscillation during 1958–2004. *Journal of Climate* **19**: 6353–6370.

Kalnay E, Kanamitsu M, Kistler R, Collins W, Deaven D, Gandin L, Iredell M, Saha S, White G, Woollen J, Zhu Y, Leetmaa A, Reynolds R. 1996. The NCEP/NCAR 40-year reanalysis project. *Bulletin of the American Meteorological Society* **77**: 437–471.

Kalnay-Rivas E, Merkine LO. 1981. A simple mechanism for blocking. *Journal of the Atmospheric Sciences* **38**: 2077–2091.

Karoly DJ. 1989. Southern hemisphere features associated with El Niño-Southern oscillation events. *Journal of Climate* **2**: 1239–1252.

Kistler R, Kalnay E, Collins W, Saha A, White G, Woollen J, Chelliah M, Ebisuzaki W, Knamitsu M, Lousky V, Dool HVD, Jenne R, Fiorino M. 2001. The NCEP-NCAR 50-year reanalysis: monthly means CD-ROM and documentation. *Bulletin of the American Meteorological Society* **82**: 247–268.

Lejenäs H. 1984. Characteristics of southern hemisphere blocking as determined from a time series of observational data. *The Quarterly Journal of the Royal Meteorological Society* **110**: 967–979.

Lejenäs H, Økland H. 1983. Characteristics of northern hemisphere blocking as determined from a long time series of observational data. *Tellus* **35A**: 350–362.

Limpasuvan V, Hartmann DL. 2000. Wave-maintained annular modes of climate variability. *Journal of Climate* **13**: 4414–4429.

Lupo AR. 1997. A diagnosis of two blocking events that occurred simultaneously in the midlatitude Northern Hemisphere. *Monthly Weather Review* **125**: 1801–1823.

Marques RF. 1996. Atmospheric blocking in the Southern Hemisphere. In *PhD dissertation*. Available at the Instituto Nacional de Pesquisas Espaciais-INPE (in Portuguese).

Marques RFC, Rao VB. 1998. A diagnosis of a long-lasting blocking event over the Southeast Pacific Ocean. *Monthly Weather Review* **127**: 1761–1776.

Marques RFC, Rao VB. 2000. Interannual variations of blocking in the Southern Hemisphere and their energetics. *Journal of Geophysical Research* **105**: 4625–4636.

Marques RFC, Rao VB. 2001. A comparison of atmospheric blockings over the southeast and southwest Pacific Ocean. *Journal of the Meteorological Society of Japan* **79**: 863–874.

Matsueda M, Hirozaku H, Mizuta R. 2010. Future change in Southern Hemisphere summertime and wintertime atmospheric blockings simulated using a 20-km-mesh AGCM. *Geophysical Research Letters* **37**: LO2803. DOI: 10.1029/2009GL041758.

Mullen SL. 1987. Transient eddy forcing and blocking flows. *Journal of the Atmospheric Sciences* **44**: 3–22.

Nakamura H, Nakamura M, Anderson JL. 1997. The role of high and low frequency dynamics in blocking formation. *Monthly Weather Review* **125**: 2074–2093.

Namias J. 1947. Extending forecasting by mean circulation methods. *U.S. Weather Bureau*, 89 pp.

Nascimento EL, Ambrizzi T. 2002. The influence of atmospheric blocking on the Rossby Wave propagation in Southern Hemisphere winter flows. *Journal of the Meteorological Society of Japan* **80**: 139–159.

Oliveira FNM. 2011. A climatology of Southern Hemisphere Blockings: observations, simulations of the 20th century and future climate change scenarios. In *Ph.D Dissertation*. Institute of Astronomy, Geophysics and Atmospheric Sciences, University of São Paulo, Brazil, 158 pp (in Portuguese).

Pelly J, Hoskins BJ. 2003. A new perspective on blocking. *Journal of the Atmospheric Sciences* **60**: 743–755.

Renwick JA. 1998. ENSO-related variability in the frequency of South Pacific Blocking. *Monthly Weather Review* **126**: 3117–3126.

Renwick JA, Revell MJ. 1999. Blocking over South Pacific and Rossby wave propagation. *Monthly Weather Review* **127**: 2233–2247.

Rex DF. 1950. Blocking action in the middle troposphere and its effect upon regional climate, part II: the climatology of blocking action. *Tellus* **2**(4): 275–301.

Rodionov SN. 2006. Use of prewhitening in climate regime shift detection. *Geophysical Research Letters* **3**(L12707): 4.

Rutllant J, Fuenzalida H. 1991. Synoptic aspects of the central Chile rainfall variability associated with the Southern Oscillation. *International Journal of Climatology* **11**: 63–76.

Shutts GJ. 1983. The propagation of eddies in diffluent jet streams: eddy vorticity forcing of blocking flow fields. *The Quarterly Journal of the Royal Meteorological Society* **109**: 737–761.

Simmonds I, Keay K. 2000. Mean southern hemisphere extratropical cyclone behavior in the 40-year NCEP–NCAR reanalysis. *Journal of Climate* **13**: 873–885.

Sinclair MR. 1996. A climatology of anticyclones and blocking for the southern hemisphere. *Monthly Weather Review* **124**: 245–263.

Smith TM, Reynolds RW, Peterson TC, Lawrimore J. 2008. Improvements to NOAA's historical merged land–ocean surface temperature analysis (1880–2006). *Journal of Climate* **21**: 2283–2296.

Thompson DWJ, Wallace JM. 2000. Annular modes in the extratropical circulation part I: month-to-month variability. *Journal of Climate* **13**: 1000–1016.

Tibaldi S, Tosi E, Navarra A, Pedulli L. 1994. Northern and southern hemisphere variability of blocking frequency and predictability. *Monthly Weather Review* **122**: 1971–2003.

Trenberth KE. 1986. An assessment of the impact of transient eddies on the zonal flow during a blocking episode using localized Eliassen-Palm flux diagnostics. *Journal of the Atmospheric Sciences* **43**(19): 2070–2087.

Trenberth KE, Mo KC. 1985. Blocking in the southern hemisphere. *Monthly Weather Review* **113**(01): 3–21.

Trigo RM, Trigo IF, DaCamara CC, Osborn TJ. 2004. Winter blocking episodes in the European–Atlantic sector: climate impacts and associated physical mechanisms in the reanalysis. *Climate Dynamics* **23**: 17–28.

Van Loon H. 1956. Blocking action in the southern hemisphere, Part I. *Notos* **5**(3): 171–175.

Wiedenmann JM, Lupo AR, Mokhov II, Tikhonova EA. 2002. The climatology of blocking anticyclones for the northern and southern hemispheres: block intensity as a diagnostic. *Journal of Climate* **15**: 3459–3473.

Wright AD. 1974. Blocking action in the Australian Region. *Department of Science Bureau of Meteorology* (Technical Report 10), 29 pp.